

# DOT1L INHIBITOR EPZ-5676: SYNTHESIS, PHARMACOKINETIC AND TISSUE DISTRIBUTION STUDIES IN SPRAGUE-DAWLEY RATS

Vijay Kumar<sup>a</sup>; Amit Kumar<sup>a</sup>; Janet W. Lightner<sup>b</sup>; Peter J. Rice<sup>a,b</sup>; Marielle Nebout<sup>c</sup>; Jean-Francois Peyron<sup>c</sup>; Michael F. Wempe<sup>a,d,\*</sup>

\* Corresponding Author: Michael F. Wempe  
Michael F. Wempe, PhD  
michael.wempe@ucdenver.edu  
(T) 303-724-8982  
(F) 303-724-6148

<sup>a</sup>Department of Pharmaceutical Sciences, School of Pharmacy, University of Colorado Denver Anschutz Medical Campus, Aurora, CO 80045, USA

<sup>b</sup>Department of Pharmacology, East Tennessee State University Johnson City, TN 37614, USA

<sup>c</sup>INSERM, U1065, Centre Méditerranéen de Médecine Moléculaire (C3M), Equipe Inflammation, Cancer, Cellules Souches Cancéreuses, Nice, France.

<sup>d</sup>University of Colorado Cancer Center, University of Colorado Denver, Aurora, Colorado 80045, USA

Email addresses, co-authors: Vijay Kumar – vijay.kumar@ucdenver.edu; Amit Kumar – amit.2.kumar@ucdenver.edu; Janet W. Lightner – lightner@mail.etsu.edu; Peter J. Rice – peter.rice@ucdenver.edu; Marielle Nebout – marielle.nebout@unice.fr; Jean-Francois Peyron – jean-francois.peyron@unice.fr.

*Keywords—Dot1L Inhibitor; EPZ-5676; Rat Pharmacokinetic Study*

---

\* Corresponding author. Tel.: 303-724-8982; fax: 303-724-6148; e-mail: michael.wempe@ucdenver.edu

Abstract—Histone methyl-transferase Dot1L can methylate histone 3 on lysine 79 (H3K79). Herein we present the chemical synthesis of a cis/trans mixture of a potent Dot1L inhibitor known as EPZ-5676 (**2**). Upon preparing compound **2**, we tested the compound in mixed and non-mixed lineage leukemia cell lines. The two *MLL*-rearranged cell lines were MV4;11 and Molm14; whereas the two non-*MLL*-rearranged (control) cell lines were Molt4 and Kasumi. We observed anticipated *in vitro* activity for compound **2** in these four leukemia cell lines; results illustrating that Dot1L inhibition can trigger cancer cell death. In addition, we also tested **2** in a new leukemia cell line known as KO99L; KO99L cells have been shown to over express the membrane amino acid transporter known as L-amino acid type 1 (LAT1). Compound **2** was also observed to decrease cell viability in the KO99L cell; albeit at higher concentrations as compared to the *MLL*-rearranged cell lines. In addition to *in vitro* experiments, we also performed *in vivo* experiments in Sprague-Dawley rats. Intravenous (*i.e.* orbital sinus dosing) experiments were performed at two different doses (*i.e.* 1.0 and 2.0 mg/kg). These rat Pharmacokinetic (PK) results indicate that compound **2** has a slow distribution phase, followed by an extended terminal half-life (*i.e.*  $11.2 \pm 3.1$  h). Furthermore, tissue distribution experiments demonstrate that **2** predominately distributes to kidney, blood and liver, and to a limited extend, was detectable in brain.

## 1. Introduction

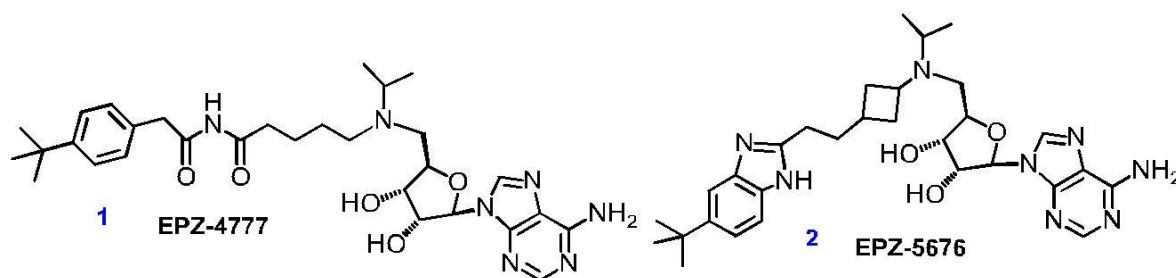
Histone methyl-transferase Dot1L methylates histone 3 on lysine 79 (H3K79) and can methylate (e.g. mono-, di- and tri-) this residue in yeast and eukaryotes (Ng et al., 2002; Van Leeuwen et al., 2002; Jones et al., 2008). Genetically modified mice illustrate that Dot1L is a specific H3K79 methyltransferase, with complete disappearance of all methylation states upon deletion of the enzyme (Jones et al., 2008). To our knowledge, there is no known H3K79 de-methylase (Nguyen et al., 2011a). Compared to most other lysine histone methyl-transferases (KMTs), Dot1L has various structurally distinct features. Most KMTs have a conserved active site with a SET domain (*Su(var)3-9*), *Enhancer of zeste* and *Trithorax*. In contrast, the Dot1L active site structurally resembles protein arginine methyl-transferases (PRMTs) (Dlakic, 2001; Min et al., 2003; Sawada et al., 2004). In yeast, Dot1's primary function is to inhibit telomeric silencing (Dot1 = "Disruptor Of Telomeric silencing-1") (Ng et al., 2002; Park et al., 2002; Sawada et al., 2004;). Ninety percent of the yeast genome gets methylated at H3K79, excluding the telomers which are silenced by a complex consisting of Sir 2, 3 and 4. Whereas, the mammalian system has only about 10% of the genome associated with H3K79 methylated histones (Jones et al., 2008). Genome-wide chromatin immunoprecipitation (ChIP) reveals that H3K79 methylations are confined to actively transcribed genes (Steger et al., 2008) and correlates with gene expression levels (Bernt et al., 2011). However, Dot1L and H3K79 methylation and their role(s) to regulate gene expression have not been fully elucidated. Dot1L has been reported to form a complex with several proteins that modulate transcriptional elongation (Bitoun et al., 2007; Mueller et al., 2007 and 2009).

Additionally, Dot1L may inhibit silencing by preventing H3K27 methylation via PRC2 (Onder et al., 2012) or de-acetylation and methylation of H3K79. The mammalian homologue of yeast Sir2 is the H3K9 deacetylase SIRT1; the de-acetylation and methylation of H3K79, as well as trimethylation of H3K27, are associated with silencing.

The first indication that Dot1L may play an important role in cancer came from a report by Okada *et al.* (Okada et al., 2005) who demonstrated that Dot1L gets recruited by leukemogenic MLL-AF10 fusion. Over the following years, it has been shown that multiple fusions of the *Mixed Lineage Leukemia (MLL)* gene are dependent on Dot1L as a downstream effector of leukemic transformation. These include MLL-AF4 (Bernt et al., 2011; Daigle et al., 2011), MLL-AF6 (Deshpande et al., 2013), MLL-AF9 (Chang et al., 2010; Jo et al., 2011; Nguyen et al. 2011c,d), MLL-AF10 (Chen et al., 2013), MLL-ENL (Daigle et al., 2011), and possibly MLL-AFX (Chang et al., 2010; Nguyen et al., 2011a,b). Furthermore, *MLL*-partial tandem duplications (*MLL-PTD*) may require functional Dot1L. Finally, leukemia triggered by the *Calm-AF10* fusion protein are Dot1L dependent and required to achieve the leukemic transformation (Min et al., 2003). In addition to Acute Myeloid Leukemia (AML), Dot1L may play a role in prostate cancer; Dot1L has been reported to directly methylate the androgen receptor, leading to enhanced androgen-receptor-mediated transcriptional activation and proliferation in prostate cancer cells (Yang et al., 2013). Dot1L deletion can be tolerated by embryonic stem (ES) cells, and *Dot1L*<sup>-/-</sup> mouse embryos appear to develop normally until day E8.5. A *Dot1L*<sup>-/-</sup> phenotype then emerges with the onset of vascular and blood development (Jones et al., 2008). In

adult animals, Dot1L is essential for early hematopoiesis (Okada et al., 2005; Nguyen et al., 2011c) as well as cardio-myocyte viability and function (Nguyen et al., 2011d). Despite early suggestions that Dot1L might regulate wnt signaling (signal transduction pathways) in the gut (Mahmoudi et al, 2010), complete absence of Dot1L in the intestine has a minimal phenotype; Dot1L does not appear to play a role in regulating intestinal homeostasis (Ho et al., 2013). Deletion or inhibition of Dot1L increases the efficiency of the reprogramming of somatic cells to induced pluripotent cells (iPS). A small molecule inhibitor of Dot1L can replace myc (a regulator gene) as a reprogramming factor. Dot1L inhibition during reprogramming appears to facilitate the repression of differentiation associated programs by Polycomb Repressive Complex 2 (PRC2) (Onder et al., 2012).

Due to the critical function of Dot1L in several highly relevant biological contexts, there has been an enormous interest and effort to develop small molecule Dot1L inhibitors. The first reported specific Dot1L inhibitor was EPZ-4777 **1** (**Figure 1**) (Daigle et al., 2011). EPZ-4777 was shown to recapitulate all key aspects of genetic inactivation by Dot1L in an MLL-AF9 mouse leukemia model. A follow-up compound with improved pharmacokinetic (PK) properties, known as EPZ-5676 **2**, was the first histone methyl-transferase to enter into a human clinical trial (NCT01684150) (Daigle et al., 2013; Basavapathruni et al., 2014). The initial dose-escalation cohorts included patients with a variety of different hematologic malignancies; an expansion cohort is currently enrolling patients specifically with *MLL*-gene fusions or *MLL-PTDs*. Several other groups have reported specific Dot1L inhibitors as well (Anglin et al., 2012; Yu et al., 2012 and 2013).

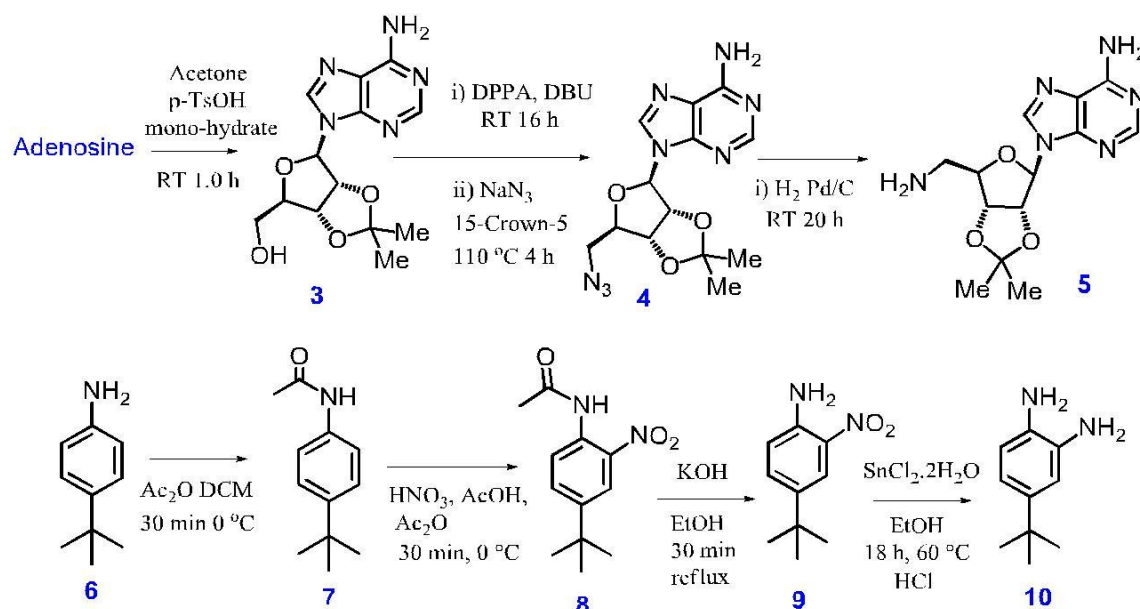
**Figure 1** Representative Dot1L inhibitors

In our ongoing efforts to evaluate potential synergistic and/or additive effects on decreased cancer cell survival regarding leukemia models (Rosilio et al., 2015), we desired to investigate the utility of a Dot1L inhibitor; consequently, we selected to use EPZ-5676 **2** as a model Dot1L inhibitor. Therefore, in the current study, we: i) performed a concise chemical synthesis to produce a cis/trans mixture of compound **2**; ii) conducted *in vitro* cell based experiments to demonstrate the inhibitory activity of **2**; iii) we developed a liquid chromatography/mass spectrometry-mass spectrometry (LC/MS-MS) method which was employed to quantitate **2** from biological fluid and tissues (*i.e.* blood, brain, liver and kidney); and iv) we performed *in vivo* experiments (Sprague-Dawley rats, SD) to generate fundamental PK and tissue distribution information which will be used to guide our dosing regimens via our *in vivo* cancer animal model experiments.

## 2. Results and Discussion

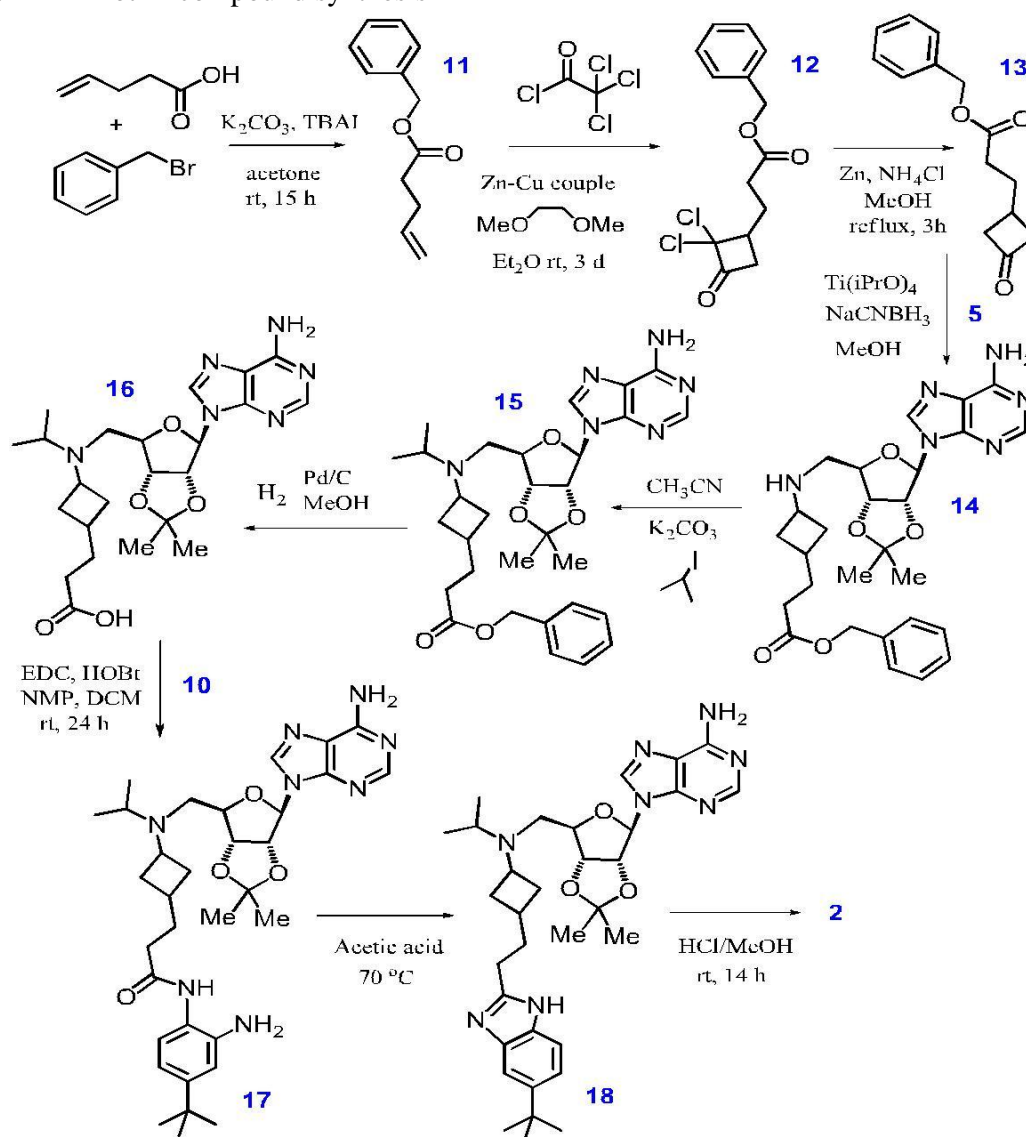
EPZ-5676 **2** (Figure 1) has been established to be an S-adenosyl methionine (SAM) competitive inhibitor of protein methyltransferase Dot1L ( $K_i = 80$  pM); **2** exhibits >37,000-fold selectivity against all other PMTs tested and inhibits H3K79 methylation in tumors. While Dot1L inhibitor **2** may be procured commercially

(*e.g.* S7062, Selleckchem) (<http://www.selleckchem.com/products/epz-5676.html>), our drug quantity requirements (*i.e.* grams) and financial constraints expanded over multiple research groups; consequently, we sought to synthesis our own drug substance. At the time when we started our work (*i.e.* 2013), some chemical synthesis information became publically available (Olhava et al., 2012); thereafter, additional information regarding alternative preparation of compound **2** was published via an additional patent application (Olhava et al., 2014). Consequently, we followed similar, but not identical synthetic pathways to prepare **2**. In order to prepare compound **2**, it required a convergent synthesis and various synthons (*i.e.* synthetic building blocks) were needed (Scheme 1). Therefore, we began with commercially available adenosine and subsequently protected the cis-diol to give ketal **3**. Next, the hydroxy functionality within **3** was converted to a good leaving group and subjected to an SN2 reaction to afford azide **4**. Azide **4** was then hydrogenated (reduced) using palladium on carbon to provide amine synthon **5**. The second required synthon was prepared by starting with aromatic amine **6** and protecting the amine as *N*-acetyl **7**. Compound **7** was subjected to nitration to give **8** which was deprotected under basic conditions to afford nitro-amine **9**. Lastly, **9** was reduced to give synthon **10**.

**Scheme 1** Synthon chemical synthesis

After preparing the two synthons (*i.e.* compound **5** and compound **10**), we proceeded with the synthesis of Dot1L inhibitor compound **2** (**Scheme 2**). Compound **2** synthesis was initiated by the base catalyzed coupling of 4-pentanoic acid with benzyl bromide to give alkene ester **11**. The cyclobutane functionality was incorporated by reacting **11** with trichloroacetyl chloride to produce dichloro **12** and subsequently reduced to cyclobutanone **13**. Next, compound **13** and synthon **5** were coupled and reduced to afford amine **14**. The secondary amine was converted to the tertiary amine **15** followed by reduction with removal of the benzyl protection group to afford carboxylic acid **16**. The diamine synthon **10** was coupled to the carboxylic acid **16** to produce amide **17**. Amide **17** was cyclized to give benzo[d]imidazole **18**. Lastly, the ketal protection group was removed to afford a cis/trans (82-83:17-18%) mixture of the desired Dot1 inhibitor **2**. In summary, we describe synthetic methods to prepare the cis/trans mixture of compound **2** in sixteen (16) chemical steps. Except for the use a benzyl ester **11**

compared to the methyl ester, and that we did not separate the cis from the trans resulting in the 4.7:1 (cis/trans) mixture, we essentially followed the same procedures as reported in a patent application (Olhava et al., 2012).

**Scheme 2** Dot1L compound synthesis

Once we had prepared Dot1L inhibitor **2**, it was imperative to demonstrate that we could observe anticipated *in vitro* activity; consequently, we probed **2** using four different cell lines (dose range 0 – 3.0  $\mu$ M; **Figure 2**) and monitored to demonstrate a dose-dependent decrease in H3K79me2 expression. These results illustrate that our cis/trans mixture of **2** exhibited concentration dependent inhibitory activity in prototypical cell lines. After confirming that **2** could influence H2K79me2 expression in a dose-dependent fashion in four different cells lines (**Figure 2**), we

sought to investigate the dose-dependent effect on cell growth in two *MLL*-rearranged cell lines (MV4;11 and Molm14), and two non-*MLL*-rearranged (control) cell lines (i.e. Molt4 and Kasumi). Cells were incubated with either no drug (control) or **2** at 0.03, 0.10, 0.30, 1.0 and 3.0  $\mu$ M (n=4) with cell growth monitored. As summarized in **Figure 3A**, inhibitor **2** produced a dose-dependent decrease in cell growth over 14 days in *MLL*-rearranged (MV4;11, Molm13) but not in the “non *MLL*-rearranged” cell lines (Kasumi, Molt4, no *MLL*-rearrangement; data not shown).

**Figure 2** MV4;11, MOLM13, MOLT4 and Kasumi cell lines dosed with Dot1L inhibitor **2** and Western blot analysis; (left) H3K27me3 protein expression, (right) H3 loading control.

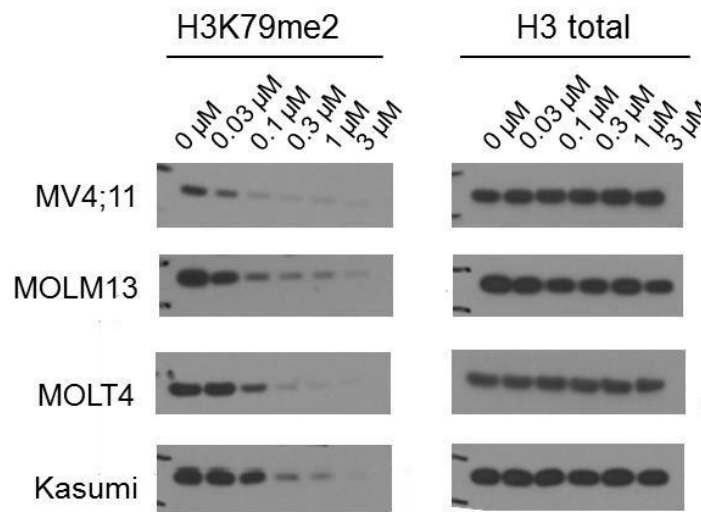
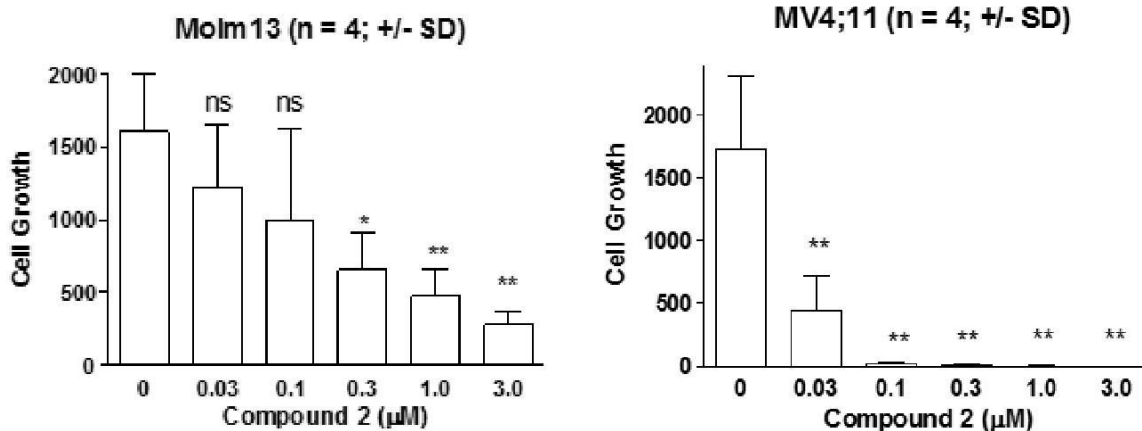


**Figure 3A:** Molm13 (*MLL-AF9*) and MV4;11 (*MLL-AF4*) were exposed to Dot1L inhibitor **2** at the indicated concentration. Cell growth is shown: control over (no drug) compared to different drug concentrations (0.03 – 3.0 μM) at culture day 14. Data n = 4 ± SD, ns = not significant; \* = p < 0.05, and \*\* = p<0.01. Molt4 and Kasumi cell lines did not display altered cell growth and are thus not presented).



These results are consistent with previously reported results which demonstrated dose dependent cell growth impediment with authentic Dot1L inhibitors (Bernt et al., 2011; Chen et al., 2015); the growth reduction was mainly attributed to a reduction in the fraction of cycling cells (**Figure 3B**). MV4;11 cells showed a significant and dose-dependent increase in apoptosis, but was not observed in Molm13, or in the control cell lines (**Figure 3C**). To

further probe the inhibitory activity of **2**, we used KO99L cell line. KO99L is a new cell line derived from a T cell lymphoma (tPTEN<sup>-/-</sup>) mouse model produced after the T-lymphocyte specific inactivation of the *PTEN* tumor suppressor gene (Rosilio et al. 2015). We have established that these KO99L cells possess elevated L-amino acid transporter 1 (LAT1) expression (Rosilio et al. 2015). LAT1 is an amino acid transporter responsible for transporting essential amino

acids (*i.e.* tyrosine, phenyl alanine, etc.) into cells. LAT1 displays selective expression in tumor cells and cancerous cells *in vivo* are strongly linked to LAT1 expression (Yanagida et al., 2001). Consequently,

cancer cells with elevated LAT1 expression are more aggressive and more resistant as compared to lower LAT1 expressing cell lines. In contrast, LAT2 is associated with normal cells (Segawa et al., 1999).

**Figure 3B:** Cell cycle analysis using EdU staining for S-phase on day 14 of compound exposure. Molm13 (*MLL-AF9*) and MV4;11 (*MLL-AF4*) were exposed to Dot1L inhibitor **2** at the indicated concentration; n = 4 ± SD, ns = not significant; \* = p < 0.05, \*\* = p < 0.01. Molt4 and Kasumi cell lines did not display altered cell growth (thus, those data are not shown).

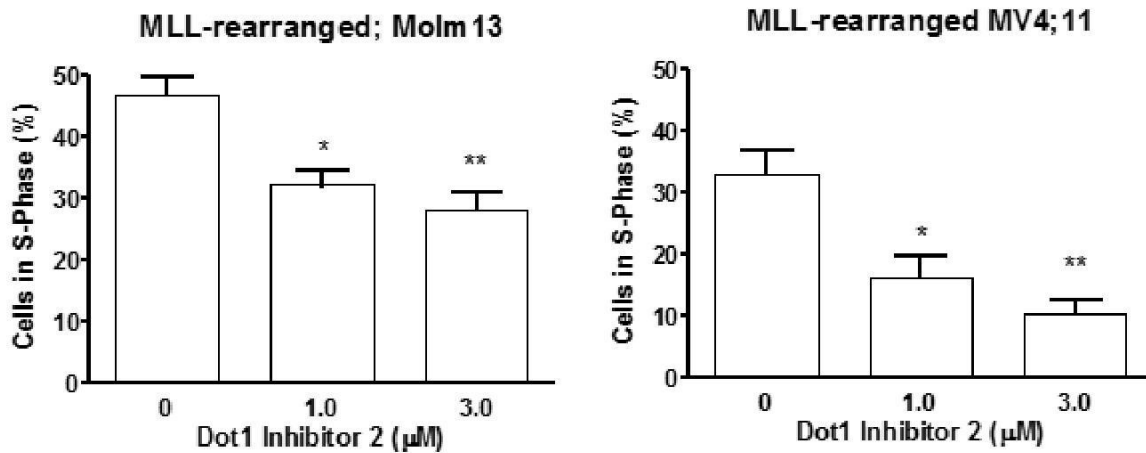
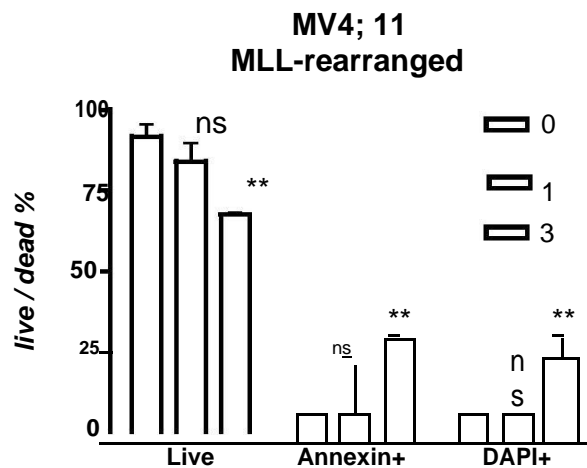


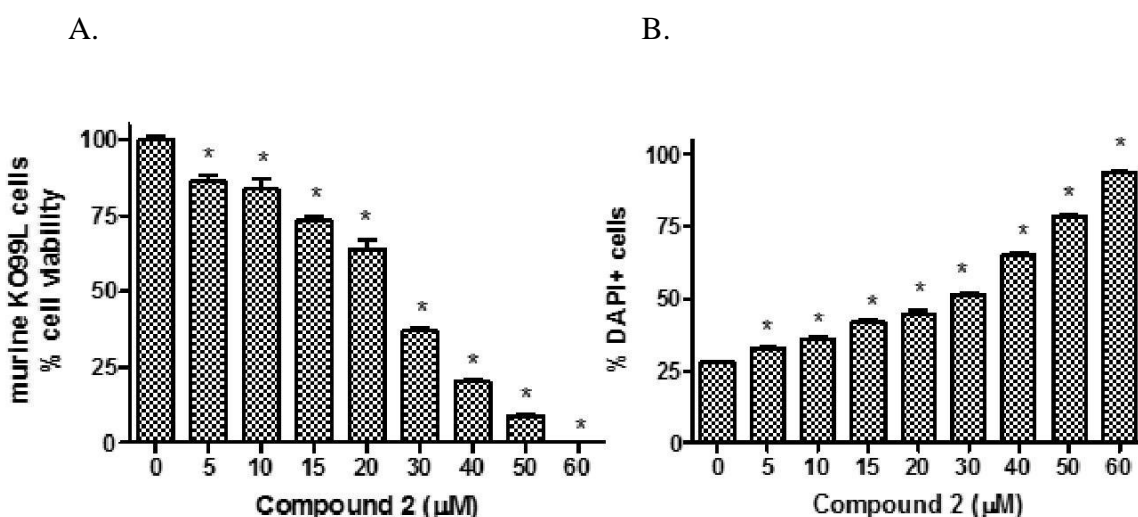
**Figure 3C:** Annexin staining to evaluate apoptosis on day 14 of compound exposure. N=3 independent experiments, error bars: SD, \*p<0.05, \*\*p<0.01



KO99L cell viability was compared in the absence and presence of various concentrations of **2**. As presented in **Figure 4A** and **Figure 4B**, cell viability was assessed by monitoring mitochondrial dehydrogenase activity and cell death (DAPI staining), respectively; the average half maximal effective concentration (EC<sub>50</sub>) was 24  $\mu$ M and 38  $\mu$ M for **Figure 4A** and **4B**, respectively. Hence, **2** displayed dose dependent *in vitro* biological activity in this

T cell lymphoma mouse cell model and presumably via its established Dot1L inhibitory properties. It is important to denote that the EC<sub>50</sub>'s are higher in cells which have elevated LAT1 expression (data not shown) and further illustrate that when cancer cells possess elevated amino acid transporter expression, that they are more resistant to prototypical drug therapy and that investigating multi-drug therapy approaches appear warranted.

**Figure 4 A:** tPTEN<sup>-/-</sup> KO99L cell line and **2** concentration dependent cell viability; n = 4  $\pm$  SD, \* = p < 0.01; **B:** tPTEN<sup>-/-</sup> KO99L cell line and **2** concentration dependent cell metabolism; n = 4  $\pm$  SD, \* = P < 0.01.



Upon completing the *in vitro* cell based work, we sought to perform *in vitro* drug metabolism studies; unfortunately, during that timeframe Basavapathruni et al. (Basavapathruni et al., 2014) published *in vitro* drug metabolism results. In rat, **2** displays low oral bioavailability with hepatic metabolism as a major route of elimination; compound **2** gets metabolized by rat liver to produce four main metabolites denoted as **M1**, **M3**, **M4** and **M6** (Basavapathruni et al., 2014). Metabolite **M1** and **M3** are via hydroxylation pathways (i.e. M + 16 amu), whereas **M4** was produced via N-dealkylation, and **M6** was

proposed to be formed via N-oxidation pathway (Basavapathruni et al., 2014). While Basavapathruni et al. (Basavapathruni et al., 2014) also performed pharmacokinetic (PK) studies, we sought to perform our own animal experiments using our produced cis/trans mixture with the goal to establish our own fundamental distribution and elimination data. Consequently, we conducted three sets of animal experiments: i) orbital sinus dosing (OSD) at a dose of 2.0 mg/kg (n = 4) with blood samples taken between 2 – to – 240 min; ii) OSD at a dose of 1.0 mg/kg (n = 4) with blood samples collected between 5 min – to – 32 hr post-

dose; and iii) OSD at a dose of 3.8 mg/kg with the animals being exterminated 1.0 hr post-dose with tissues harvested. To establish sound bioanalytical methods, we prepared LC/MS-MS standard curves using nine standard curve concentrations ( $n = 4$ ) which represented concentrations between 0.8 – 2812 ng/mL. A standard curve was prepared for each: brain, blood, kidney, and liver. The limit of detection (LOD) values were  $\leq 0.2$  ng/mL (ng/g tissue) while the limit of quantitation (LOQ) values were approximately 0.3 ng/mL (blood) and 0.7 ng/g for tissue homogenates. Standard curve data were fitted to a  $1/x^2$  weighted linear regressions; brain, blood, kidney, and liver standard curves displayed correlation coefficients ( $R^2$ ) of 0.9916, 0.9984, 0.9918, and 0.9949, respectively.

### Conclusions

Olhave et al. (Olhave et al., 2014) have demonstrated that Dot1L inhibitor **2** has the ability to decrease tumor volume growth and therefore one method to treat leukemia in an animal model. In **Figure 5A** we present the results from our PK experiments – dosed at 2.0 mg/kg (OSD) – which illustrated a slow and extended distribution (0 – 90 min) of compound **2**. This long distribution phase began to level off between 120 – 240 min post-dose. These data are consistent with an open multi-compartmental model rather than a situation where the OSD instantly distributes (i.e. equilibrates) between blood and tissues. The PK values computed from the 2.0 mg/kg dose data produced the following values:  $T_{max} = 0.31 \pm 0.18$  h,  $C_{max} = 1493 \pm 149$  ng/mL, elimination  $T_{1/2} 2.9 \pm 0.9$  h, and  $AUC_{0-\infty} = 3016 \pm 253$  h•ng/mL. While we collected and analyzed blood, not plasma, these PK data, namely  $T_{1/2}$  data, are consistent with results reported by Basavapathruni et al. (Basavapathruni et al., 2014). However, as

these rat data did not provide sufficient post-dose time-point data, we felt that these data could not adequately establish the terminal elimination half-life. Consequently, a second set of OSD experiments was performed. As summarized in **Figure 5B**, we dosed **2** at 1.0 mg/kg and collected blood samples from 0.083 – 32 h post-dose. The data from these experiments (i.e. the last nine time points) provided sufficient data to compute a terminal elimination half-life. As per the 2.0 mg/kg dose (**Figure 5A**), the 1.0 mg/kg dose also displayed (**Figure 5B**) a long and slow distribution phase. The computed PK values from these data produced the following results:  $T_{max} = 0.17 \pm 0.10$  h,  $C_{max} = 717 \pm 66$  ng/mL, elimination  $T_{1/2} 11.2 \pm 3.1$  h, and an  $AUC_{0-\infty} = 349 \pm 74$  h•ng/mL. Hence, having sufficient time-point data helps to illustrate the long elimination  $T_{1/2}$  of **2** and that rat and dog (Basavapathruni et al., 2014), in our opinion, are not different but are really rather similar. Lastly, we performed an OSD experiment (3.8 mg/kg) – but terminated the experiment approximately one hour post-dose – and collected blood and tissues (brain, liver and kidneys). As summarized in **Figure 5C**, compound **2** was observed to distribute (equilibrate) between the blood compartment and the kidneys and liver. These tissue distribution data suggest that **2** can cross the blood-brain barrier (BBB), albeit the observed brain drug concentrations were marginal ( $23 \pm 10$  ng/g tissue). In summary, our LC/MS-MS methods and these PK and tissue distribution data provide vital ADME information which we will use to guide dosing (dose and frequency) in our leukemia and renal cancer *in vivo* cancer models. Having established the PK and tissue distribution data in rats for the potent LAT1 inhibitor known as JPH203 (Wempe et al., 2012), and now (herein) establishing our own in-house synthesis and

PK/PD information regarding **2**, we can now rationally proceed with in-house in vivo experiments to test multi-drug therapy approaches to better combat cancer. These experiments will be conducted in the presence and absence of the potent LAT1 inhibitor(s) JPH203 with the aim to establish, or not, *in vivo* synergistic effects which are predicted via *in vitro* cell data (i.e. we want to probe and establish in vitro – in vivo correlations, IV-IV). While the Dot1L inhibitor **2** is an interesting compound, it is important to mention that **2** suffers from poor bioavailability, rapid clearance and thus requires the clinical implementation of

a continuous intravenous administration. Hence, additional research in our laboratories regarding formulation development and multi-drug cocktails for use as novel drug therapy is warranted and a goal of current research in our laboratories. The chemical synthesis presented herein and the experimental results from the current studies demonstrate that the cis/trans mixture of **2** behaves very similar to pure cis; consequently, we believe that the cis/trans mixture can be used as a chemical probe to successfully perform non-clinical experiments.

**Figure 5 A:** OSD of **2** (2.0 mg/kg), blood versus time (5 – 240 min),  $n = 4 \pm SD$ ; **B:** OSD of **2** (1.0 mg/kg), blood versus time (0.083 – 32 h),  $n = 4 \pm SD$

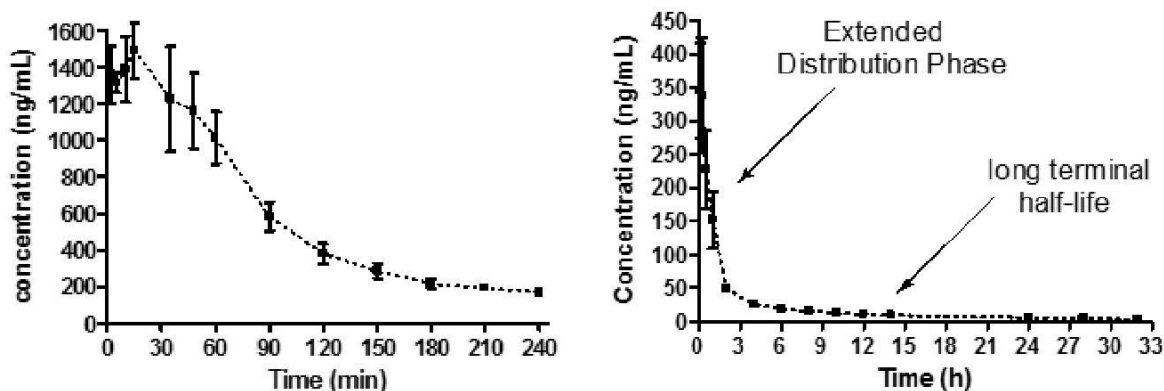
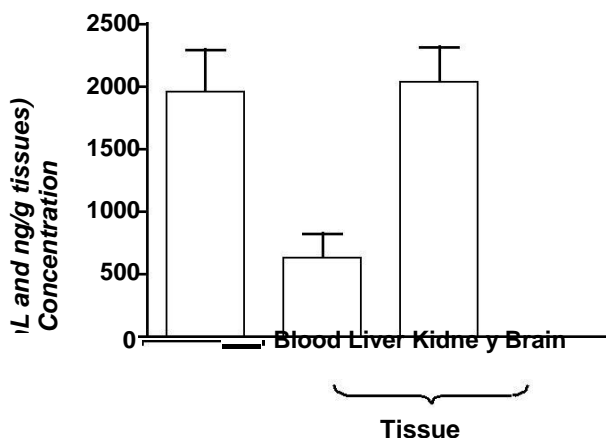


**Figure 5C.** OSD of **2** (3.8 mg/kg), 1.0 h post-dose, blood and tissue concentrations,  $n = 4 \pm SD$



### Materials and Methods

Acetic acid, acetic anhydride, anhydrous acetone, acetonitrile (ACN), alumina, ammonium chloride, ammonium acetate, diethyl ether, dimethyl sulfoxide (DMSO), 1,2-dimethoxyethane, 1,4-dioxane, ethyl acetate (EtOAc), formic acid, hexanes, hydrochloric acid (HCl), methanol (MeOH), methylene chloride (DCM), nitric acid, potassium carbonate (K<sub>2</sub>CO<sub>3</sub>), potassium hydroxide (KOH), sodium bicarbonate (NaHCO<sub>3</sub>), sodium chloride (NaCl), sodium hydroxide (NaOH), anhydrous sodium sulfate (Na<sub>2</sub>SO<sub>4</sub>), *p*-toluene-sulfonic acid monohydrate (TsOH H<sub>2</sub>O), triethyl amine (TEA), HPLC grade water (H<sub>2</sub>O), and zinc were purchased from Fisher Scientific (Pittsburgh, PA). Celite, deuterated chloroform (CDCl<sub>3</sub>), deuterated dimethyl sulfoxide (DMSO-*d*<sub>6</sub>), 4-pentanoic acid, benzyl bromide, tetrabutylammonium iodide (TBAI), zinc-copper (Zn-Cu) couple, trichloroacetyl chloride (TCAC), Ti(iPrO)<sub>4</sub>, sodium cyano-borohydride (NaCNBH<sub>3</sub>), 2-iodopropane, 10% Pd on Carbon (Pd/C), 4-tert-butyl-2-nitroaniline, stannous chloride dehydrate (EDCI), 1-hydroxy-7-azabenzotriazole (HOAT), hydrochloric acid lecture bottle, nitric acid, adenosine, DPPA, DBU, sodium azide (NaN<sub>3</sub>), and 15-crown-5, were purchased from Sigma-Aldrich Chemical Company (St. Louis, MO). Nitrogen gas and hydrogen gas were procured from AirGas<sup>®</sup> (Denver, CO). Ethanol was purchased from Decon Laboratories, Inc. (King of Prussia, PA). Reactions were monitored via silica gel IB2-F thin layer chromatography (TLC) plates from J.T. Baker (Phillipsburg, NJ). Silica Gel 60 Å 40-63 μm was purchased from Sorbent Technologies (Norcross, GA). Control tissues – male rat whole blood (K<sub>2</sub> EDTA), livers, kidneys, and brains – were purchased from Bioreclamation LLC (Westbury, NY). The NMR spectra were recorded using a 400 MHz Bruker NMR, Avance III 400. The chemical shifts are

reported in ppm. An Applied Biosystems Sciex 4000 (Applied Biosystems; Foster City, CA) equipped with a Shimadzu HPLC (Shimadzu Scientific Instruments, Inc.; Columbia, MD) and Leap auto-sampler (LEAP Technologies; Carrboro, NC) was used to implement the BioAnalytical Pharmacokinetic (BAPK) analysis.

### Chemical Synthesis

#### Preparation of 9-((3*aR*,4*R*,6*R*,6*aR*)-6-(aminomethyl)-2,2-dimethyltetrahydrofuro[3,4-*d*][1,3]dioxol-4-yl)-9*H*-purin-6-amine (**5**; Scheme 1)

((3*aR*,4*R*,6*R*,6*aR*)-6-(6-*amino*-9*H*-purin-9-yl)-2,2-dimethyltetrahydrofuro[3,4-*d*][1,3]dioxol-4-yl)methanol **3**: Adenosine (10.0 g, 37.4 mmol) was suspended in acetone (2.0 L) followed by the addition of TsOH monohydrate (71.2 g, 374 mmol). Next, the reaction mixture was stirred under a N<sub>2</sub> atmosphere (nitrogen balloon); the solution turned yellow upon dissolving. After stirring (12 h), saturated ice cold NaHCO<sub>3</sub> aq. (500 mL) was added with stirring over 20 min. The mixture was concentrated under reduced pressure and resulting solid stirred in acetone (0.5 L; 18 h) and Büchner filtered. The solvent was evaporated and the crude product was purified by silica gel (SiO<sub>2</sub>) column chromatography (dichloromethane/methanol 10:1). The desired product fractions were combined, concentrated and dried under vacuum to afford (**3**; 6.01 g; 52% yield). <sup>1</sup>H-NMR (400 MHz, CDCl<sub>3</sub>): δ 8.32 (s, 1H), 7.83 (s, 1H), 6.56–6.49 (m, 1H), 5.88–5.72 (m, 3H), 5.22–5.18 (m, 1H), 5.13–5.10 (m, 1H), 4.54 (br s, 1H), 4.00–3.95 (m, 1H), 3.83–3.75 (m, 1H), 1.65 (s, 3H) and 1.37 (s, 3H) ppm.

9-((3*aR*,4*R*,6*R*,6*aR*)-6-(azidomethyl)-2,2-dimethyltetrahydrofuro[3,4-*d*][1,3]dioxol-4-yl)-9*H*-purin-6-amine **4**: To a stirred solution of 1,4 dioxane (100 mL), 2',3'-O-isopropylideneadenosine (**3**, 10.0 g, 32.5 mmol) was added; next DPPA (14.0 mL,

65.1 mmol) and DBU (14.6 mL, 97.7 mmol) were added at room temperature under N<sub>2</sub>. The solution was stirred (16 h) and NaN<sub>3</sub> (10.6 g, 163 mmol) and 15-crown-5 (65.0 μL, 0.330 mmol) were added. The mixture was heated (reflux; 4 h), allowed to cool to ambient temperature, and solids removed via Büchner filtration. The filtrate was concentrated under reduced pressure and purified via column chromatography (ethyl acetate/ methanol 19:1, SiO<sub>2</sub>). After drying under high vacuum, it produced colorless solid (**4**; 8.20 g; 76% yield). <sup>1</sup>H-NMR (400 MHz, CDCl<sub>3</sub>): δ 8.36 (s, 1H), 7.91 (s, 1H), 6.12–6.09 (m, 1H), 5.58 (br s, 2H), 5.48–5.44 (m, 1H), 5.08–5.04 (m, 1H), 4.40–4.35 (m, 1H), 3.63–3.53 (m, 2H), 1.62 (s, 3H) and 1.39 (s, 3H) ppm.

*9-((3aR,4R,6R,6aR)-6-(aminomethyl)-2,2-dimethyltetrahydrofuro[3,4-d][1,3]dioxol-4-yl)-9H-purin-6-amine* **5**: Into a Parr container, compound (**4**, 8.00 g, 24.1 mmol) was dissolved in EtOH (250 mL) and 10 % Pd/C (800 mg) added. The reaction mixture was placed under H<sub>2</sub> (3 bar) and shaken at RT (24 h). The mixture was filtered through celite and the filtrate concentrated under reduced pressure and vacuum-line dried to afford off-white solid (6.80 g, 92 % yield). <sup>1</sup>H-NMR (400 MHz, DMSO *d*<sub>6</sub>): δ 8.34 (s, 1H), 8.13 (s, 1H), 7.28 (br s, 2H), 6.07–6.02 (m, 1H), 5.44–5.38 (m, 1H), 4.98–4.92 (m, 1H), 4.10–4.03 (m, 1H), 2.72–2.61 (m, 2H), 1.57 (s, 3H) and 1.30 (s, 3H) ppm.

*N-(4-(tert-butyl)phenyl)acetamide* **7**: To an ice-cold solution of 4-tert-butylaniline (**6**, 5.00 g, 33.5 mmol) in DCM (25 mL) was slowly added acetic anhydride (3.5 mL, 37.1 mmol). The reaction mixture was stirred (30 min) to produce colorless solid product under air, during which colorless plates formed. The mixture was concentrated *in vacuo* and hexane added to further generate precipitate which was collected by Büchner filtration and washed with hexanes, to give colorless plates of (**5**; 6.00 g, 97% yield). <sup>1</sup>H-NMR (400 MHz, CDCl<sub>3</sub>): δ 7.43–7.38

(m, 2H), 7.35– 7.31 (m, 2H), 2.16 (s, 3H) and 1.30 (s, 9H) ppm.

*N-(4-(tert-butyl)-2-nitrophenyl)acetamide* **8**: To an ice-cold stirring mixture of acetic acid (9.5 mL, 164 mmol) and acetic anhydride (8.0 mL, 84 mmol) was added nitric acid (70%, 3.0 mL). After 5.0 min, (**7**, 1.0 g, 5.2 mmol) was added to this mixture and in portions. The reaction mixture was further stirred (ice-cold, 30 min). HPLC grade ice cold water was slowly added to quench the reaction, which was kept in an ice bath. The quenched reaction mixture was subjected to further addition of water to produce a yellow precipitate. The precipitate was collected via Büchner filtration, washed with cold water and dried to give yellow solid (**8**, 900 mg, 73% yield). <sup>1</sup>H-NMR (400 MHz, CDCl<sub>3</sub>): δ 10.3–10.1 (br s, 1H), 8.66–8.61 (m, 1H), 8.19–8.16 (m, 1H), 7.70–7.65 (m, 1H), 2.28 (s, 3H) and 1.34 (s, 9H) ppm.

*4-(tert-butyl)-2-nitroaniline* **9**: To an ethanolic (5.0 mL) solution of (**8**, 1.00 g, 4.24 mmol) was added KOH pellets (258 mg, 4.67 mmol) and heated to reflux (30 min). Next, the mixture was poured into ice-cold water (150 mL). The resulting precipitate was Büchner filtered, washed with cold water, and dried *in vacuo* to give orange solid (**9**; 750 mg, 91% yield). <sup>1</sup>H-NMR (400 MHz, CDCl<sub>3</sub>): δ 8.11–8.06 (m, 1H), 7.46–7.39 (m, 1H), 6.76 (d, *J* = 8.5 Hz, 1H), 6.01–5.85 (br s, 2H) and 1.31–1.27 (m, 9H) ppm.

*4-(tert-butyl)benzene-1,2-diamine* **10**: To an ethanolic solution (10 mL) of 4-tert-butyl-2-nitroaniline (**9**; 100 mg, 0.51 mmol), conc. HCl (1.0 mL) was added followed by stannous chloride dihydrate (697 mg, 3.08 mmol). The reaction was stirred under N<sub>2</sub> (60 °C, 18 h). Water was then added and the mixture poured into a stirring aqueous solution of NaOH (3.0 M), resulting in the formation of a white precipitate. Saturated NaHCO<sub>3</sub> aq. solution was added and pH adjusted to ~8. DCM (50 mL) was added and the mixture was stirred (5 min) and the

white precipitate collected by filtration. The combined organic phases were washed with brine, dried over anhydrous Na<sub>2</sub>SO<sub>4</sub>, filtered and concentrated to give (**10**, 60 mg, 71% yield) as a white solid. Note: the product is unstable in air and decomposes to a brown solid over days (decomposition occurs much faster in solution); hence we recommend that compound **10** be prepared immediately prior to use. <sup>1</sup>H-NMR (400 MHz, CDCl<sub>3</sub>): δ 6.77-6.71 (m, 2H), 6.67-6.62 (m, 1H), 3.44-3.24 (m, 4H) and 1.27-1.26 (m, 9H) ppm.

### Preparation of EPZ-5676 **2**; (Scheme 2)

*Benzyl pent-4-enoate* **11**: Benzyl bromide (14.2 mL, 120 mmol) was added to a solution of 4-pentanoic acid (10.3 mL, 99.9 mmol) in dry acetone (200 mL) containing potassium carbonate (69.0 g, 499 mmol) and tetrabutylammonium iodide (3.69 g, 9.99 mmol). Upon addition and stirring (15 h), the reaction mixture was Büchner filtered and filtrate concentrated under reduced pressure. This material was then dissolved in ethyl acetate (100 mL), washed with 2.0 M HCl aq (60 mL), sat. NaHCO<sub>3</sub> aq (50 mL), brine (50 mL) and then dried over anhydrous Na<sub>2</sub>SO<sub>4</sub>. The material was filtered and the filtrate concentrated and purified by SiO<sub>2</sub> column chromatography (MeOH/DCM) to afford (**11**, 95% yield) as colorless oil. <sup>1</sup>H-NMR (CDCl<sub>3</sub>, 400 MHz): δ 7.40-7.32 (m, 5H), 5.86-5.77 (m, 1H), 5.13 (s, 2H), 5.09-4.98 (m, 2H), 2.49-2.49 (m, 2H) and 2.43-2.37 (m, 2H) ppm.

*Benzyl 3-(2,2-dichloro-3-oxocyclobutyl)propanoate* **12**: A mixture of benzyl pent-4-enoate (**11**; 5.00 g, 26.3 mmol) and Zn-Cu couple (4.3 mg, 67 mmol) in Et<sub>2</sub>O (100 mL) and 1,2-dimethoxyethane (10 mL) treated drop-wise with trichloroacetyl chloride (7.5 mL, 67 mmol). The reaction mixture was capped and stirred at RT (3 days). The reddish heterogeneous reaction mixture was filtered through a

Celite pad with the pad being washed with EtOAc, followed by water and sat. NaHCO<sub>3</sub> aq. The organic phase was then concentrated under reduced pressure and purified by SiO<sub>2</sub> silica gel column chromatography (hexanes-DCM) to give (**12**, 6.30 g, 80% yield) as a yellow liquid. <sup>1</sup>H-NMR (CDCl<sub>3</sub>, 400 MHz): δ 7.37-7.30 (m, 5H), 5.10 (s, 2H), 3.18-3.10 (m, 1H), 2.73-2.65 (m, 1H), 2.43-2.35 (m, 2H), 2.34-2.28 (m, 1H) and 1.80-1.70 (m, 2H) ppm.

*Benzyl 3-(3-oxocyclobutyl)propanoate* **13**: To a stirred solution of (**12**; 13.5 g, 44.8 mmol) in MeOH (200 mL) was added ammonium chloride (12.0 g, 224 mmol) and zinc powder (14.7 g, 224 mmol). The reaction mixture was refluxed (3.0 h). After cooling to ambient temperature, the mixture was filtered through a plug of Celite and washed with EtOAc. The filtrate was then washed with sat. NaHCO<sub>3</sub> aq., mixed and the organic phase concentrated under reduced pressure. The crude material was then purified via SiO<sub>2</sub> column chromatography eluting with hexanes-DCM to give **13** (6.20 g, 60% yield) as a liquid. <sup>1</sup>H-NMR (CDCl<sub>3</sub>, 400 MHz): δ 7.37-7.34 (m, 5H), 5.17 (s, 2H), 3.36-3.29 (m, 1H), 3.04-2.92 (m, 2H), 2.63-2.49 (m, 3H), 2.26-2.14 (m, 2H) and 2.08-2.01 (m, 1H) ppm.

*Benzyl 3-(3-(((3aR,4R,6R,6aR)-6-(6-amino-9H-purin-9-yl)-2,2-dimethyltetrahydrofuro[3,4-d][1,3]dioxol-4-yl)methyl)amino)cyclobutyl)propanoate* **14**: A methanolic solution (30 mL) containing (**5**, 3.82 g, 12.5 mmol), benzyl 3-(3-oxocyclobutyl)propanoate (**13**, 2.90 g, 12.5 mmol), and Ti(iPrO)<sub>4</sub> (3.55 g, 12.5 mmol) was stirred (45 °C for 2.0 h) and then NaCNBH<sub>3</sub> (1.57 g, 25.0 mmol) added in portions. The reaction was stirred overnight at RT and then quenched with sat. NaHCO<sub>3</sub> aq. (25 mL), and extracted with DCM (100 mL × 3). The organic phase was dried over anhydrous Na<sub>2</sub>SO<sub>4</sub>, filtered and concentrated. The residue was then purified by SiO<sub>2</sub> column (DCM:MeOH = 10:1) to afford diastereo-isomers, cis/trans (17-

18:82-83%) mixture (**14**, 2.20 g, yield 34%). <sup>1</sup>H-NMR (400 MHz, CDCl<sub>3</sub>): δ 8.36–8.31 (m, 1H), 7.92–7.88 (m, 1H), 7.39–7.28 (m, 5H), 6.02–5.98 (m, 1H), 5.77–5.65 (m, 2H), 5.52–5.45 (m, 1H), 5.12–5.06 (m, 2H), 5.04–4.96 (m, 1H), 4.37–4.29 (m, 1H), 3.34–3.24 (m, 0.35H), 3.08–2.96 (m, 1.65H), 2.86–2.69 (m, 2H), 2.36–2.06 (m, 4H), 1.92–1.56 (m, 8H), 1.36 (s, 3H) and 1.25–1.08 (m, 1H) ppm.

*Benzyl 3-(3-(((3aR,4R,6R,6aR)-6-(6-amino-9H-purin-9-yl)-2,2-dimethyltetrahydrofuro[3,4-d][1,3]dioxol-4-yl)methyl)(isopropyl)amino)cyclobutyl)propanoate* **15**: To (**14**, 2.10 g, 4.02 mmol) in CH<sub>3</sub>CN (15 mL) was added 2-iodopropane (4.1 g, 24 mmol) and anhydrous K<sub>2</sub>CO<sub>3</sub> (1.11 g). The reaction was heated (95 °C; 14 h) in a sealed tube. The reaction mixture was cooled to ambient temperature, filtered, and the filtrate concentrated under reduced pressure to give (**15**, 1.8 g, Yield 87%) as a diastereomeric (cis/trans) mixture. <sup>1</sup>H-NMR (400 MHz, CDCl<sub>3</sub>): δ 8.37–8.32 (m, 1H), 7.92–7.84 (m, 1H), 7.40–7.28 (m, 5H), 6.07–5.98 (m, 1H), 5.76 (br s, 2H), 5.53–5.48 (m, 1H), 5.13–5.06 (m, 1H), 5.02–4.94 (m, 1H), 4.35–4.22 (m, 1H), 3.42–3.32 (m, 0.35H), 3.06–2.88 (m, 1.65H), 2.77–2.62 (m, 1H), 2.58–2.46 (m, 1H), 2.32–2.04 (m, 4H), 1.84–1.54 (m, 7H), 1.48–1.22 (m, 5H), 1.02–0.92 (m, 3H) and 0.82–0.72 (m, 3H) ppm.

*3-(3-(((3aR,4R,6R,6aR)-6-(6-amino-9H-purin-9-yl)-2,2-dimethyltetrahydrofuro[3,4-d][1,3]dioxol-4-yl)methyl)(isopropyl)amino)cyclobutyl)propanoic acid* **16**: Compound (**15**, 1.80 g, 3.19 mmol) was transferred to a Parr hydrogenation vessel and dissolved in MeOH (30 mL) followed by 10 % Pd/C (500 mg). The reaction mixture was placed under H<sub>2</sub> (3 bar; 40 h). Afterwards, the reaction mixture was filtered through a plug of celite and the filtrate evaporated and purified by SiO<sub>2</sub> column chromatography (1:3:16 = NH<sub>4</sub>OH:MeOH:DCM) to give (**16**, 600 mg, 40% yield) as a diastereomeric mixture. <sup>1</sup>H-NMR (400 MHz,

CDCl<sub>3</sub>): δ 8.32–8.26 (m, 1H), 7.99–7.93 (m, 1H), 6.93–6.74 (m, 2H), 6.07–6.01 (m, 1H), 5.56–5.50 (m, 1H), 5.04–4.96 (m, 1H), 4.34–4.26 (m, 1H), 3.44–3.34 (m, 0.34H), 3.10–2.91 (m, 1.66H), 2.78–2.64 (m, 1H), 2.62–2.48 (m, 1H), 2.26–2.11 (m, 2H), 2.07–1.83 (m, 2H), 1.80–1.50 (m, 7H), 1.43–1.31 (m, 4H), 1.05–0.94 (m, 3H) and 0.93–0.83 (m, 3H) ppm.

*N-(2-amino-4-(tert-butyl)phenyl)-3-(3-(((3aR,4R,6R,6aR)-6-(6-amino-9H-purin-9-yl)-2,2-dimethyltetrahydrofuro[3,4-d][1,3]dioxol-4-yl)methyl)(isopropyl)amino)cyclobutyl)propanamide* **17**: To a stirred solution of (**16**, 120 mg) in DCM (10 mL) was added (**10**, 82.1 mg), EDCI (95.6 mg), HOBT (67.6 mg) and TEA (200 mg) at room temperature. The reaction mixture was stirred at RT (14 h) and then concentrated under reduced pressure. Next, sat. NaHCO<sub>3</sub> aq. (10 mL) was added and the mixture extracted with DCM. The organic layers were dried over anhydrous Na<sub>2</sub>SO<sub>4</sub>, filtered and concentrated. The crude material was purified using neutral alumina column chromatography (DCM:MeOH = 97:3) to afford (**17**, 60 mg, 39% yield, cis/trans mixture). <sup>1</sup>H-NMR (400 MHz, CDCl<sub>3</sub>): δ 8.42–8.32 (m, 1H), 7.96–7.78 (m, 2H), 7.38–7.05 (m, 1H), 6.88–6.62 (m, 2H), 6.08–6.00 (m, 1H), 5.88–5.48 (m, 3H), 5.05–4.05 (m, 1H), 4.36–3.76 (m, 3H), 3.42–3.28 (m, 0.35H), 3.08–2.85 (m, 1.65H), 2.78–2.46 (m, 2H), 2.28–1.54 (m, 10H), 1.39 (s, 3H), 1.32–1.16 (m, 9H), 1.04–0.92 (m, 3H) and 0.90–0.78 (m, 3H) ppm.

*9-(((3aR,4R,6R,6aR)-6-(((3-(2-(5-(tert-butyl)-1H-benzo[d]imidazol-2-yl)ethyl)cyclobutyl)(isopropyl)amino)methyl)-2,2-dimethyltetrahydrofuro[3,4-d][1,3]dioxol-4-yl)-9H-purin-6-amine* **18**: Compound (**17**, 60 mg, 0.10 mmol) was dissolved in acetic acid (10 mL) and heated (70 °C, 14 h). Next, the mixture was cooled to ambient temperature and concentrated under reduced pressure and sat. NaHCO<sub>3</sub>

solution (10 mL) added. The mixture was extracted with DCM. The organic phase was dried over anhydrous Na<sub>2</sub>SO<sub>4</sub>, filtered, and concentrated to give (**18**, 50 mg, 83% yield; cis/trans mixture). <sup>1</sup>H-NMR (400 MHz, CDCl<sub>3</sub>): δ 10.70–10.45 (m, 0.64H), 9.92–9.71 (m, 0.36H), 8.46–8.33 (m, 1H), 7.99–7.89 (m, 1H), 7.77–7.56 (m, 1H), 7.50–7.35 (m, 1H), 7.33–7.26 (m, 1H), 6.11–6.03 (m, 1H), 5.77–5.54 (m, 3H), 5.07–4.97 (m, 1H), 4.31–4.24 (m, 1H), 3.38–3.28 (m, 0.36H), 3.07–2.85 (m, 1.64H), 2.76–2.46 (m, 2H), 2.08–1.51 (m, 10H), 1.44–1.34 (m, 12H), 1.28–1.06 (m, 2H) 1.00–0.92 (m, 3H) and 0.89–0.77 (m, 3H) ppm.

(2*R*,3*R*,4*S*,5*R*)-2-(6-amino-9*H*-purin-9-yl)-5-(((3-(2-(5-(*tert*-butyl)-1*H*-benzo[*d*]imidazol-2-yl)ethyl)cyclobutyl)(isopropyl)amino)methyl)tetrahydrofuran-3,4-diol **2**: A solution of (**18**, 55 mg, 0.09 mmol) in HCl/MeOH (0.5 M, 10 mL) was stirred at RT (14 h) and then concentrated under reduced pressure. Next, K<sub>2</sub>CO<sub>3</sub> (50 mg) in water (0.5 mL) and MeOH (5.0 mL) were added and mixture stirred (2.0 h) at RT. The material was then concentrated and filtered with cold MeOH to give (**2**; cis/trans mixture, 40 mg, 79% yield) as an off white solid. <sup>1</sup>H-NMR (400 MHz, MeOD): δ 8.31–8.27 (m, 1H), 8.20–8.17 (m, 1H), 7.49–7.45 (m, 1H), 7.40–7.34 (m, 1H), 7.29–7.23 (m, 1H), 5.97–5.93 (m, 1H), 4.75–4.70 (m, 1H), 4.28–4.22 (m, 1H), 4.10–4.03 (m, 1H), 3.57–3.50 (m, 0.36H), 3.17–3.07 (m, 0.64H), 3.05–2.65 (m, 5H), 2.21–2.10 (m, 2H), 2.07–1.72 (m, 4H), 1.61–1.50 (m, 1H), 1.38–1.32 (m, 9H) 1.05–0.97 (m, 3H) and 0.96–0.89 (m, 3H) ppm. <sup>13</sup>C NMR (100 MHz, MeOD): δ 160.0, 155.9, 155.2, 155.1, 152.4, 149.2, 145.2, 140.3, 137.9, 136.2, 119.7, 119.3, 113.4, 109.9, 89.1, 83.7, 83.6, 73.3, 72.1, 72.1, 53.5, 52.5, 50.1, 49.9, 49.2, 48.9, 35.0, 35.0, 34.9, 34.2, 33.9, 32.5, 30.9, 28.2, 27.7, 26.9, 26.3, 17.9, 17.7, 17.0, 16.9 ppm. Large Scale example: A solution of imidazole (**18**,

1.60 g, 2.66 mmol) in HCl/MeOH (0.5 M, 40 mL) was stirred at rt (15 h) and then concentrated to dryness. K<sub>2</sub>CO<sub>3</sub> (800 mg) in water (5 mL) and MeOH (15 mL) were added and the reaction mixture was stirred for another 2 h at room temperature. Next. The mixture was concentrated to dryness and filtered to give **2** (cis/trans mixture, 1.20 g, 80% yield) as an off white solid.

### *In vitro* Biological Activity

The following human cell lines were obtained from *American Type Culture collection*: MV-4;11 (ATCC CRL-9591), Molt-4 (ATCC-1582). The following cell lines were purchased from the *Deutsche Sammlung von Mikroorganismen und Zellkulturen* (DSMZ, Germany): MOLM-14 (DMSZ ACC 554), KASUMI-1 (DMSZ ACC 220). All cells were maintained in RPMI-1640 media (Invitrogen) supplemented with heat-inactivated 10% fetal bovine serum, 2.0 mM L-glutamine, non-essential amino acids and 50 U/mL Penicillin/Streptomycin (all Gibco, Invitrogen, Carlsbad, CA). All cells were cultured in the appropriate medium in a humidified incubator at 37 °C (5% CO<sub>2</sub>). Cell growth and viability were followed by serial cell counts and trypan blue exclusion staining. Cells (50,000 well) were plated in the indicated concentrations of compound **2** at equal concentrations of solvent (DMSO, 0.04%). Cells were re-plated at 50,000 cells in fresh media with compound **2** every 2-4 d. Cell numbers were recorded, and the fold-expansion compared to DMSO control was calculated at the end, culture day 14.

For the annexin V apoptosis assay, cells exposed to Dot1L inhibitor **2** at the indicated drug concentration for 14 d were washed in PBS, re-suspended in Ca/HEPES buffer (10 mM HEPES, pH 7.4; 140 mM NaCl; 2.5 mM CaCl<sub>2</sub>) and incubated (30 min) with Annexin V-APC (Pharmingen, San Jose, CA). DAPI was added prior to analysis. Cell

cycle analysis was performed after EDU labeling for 30 min after being exposed to Dot1L inhibitor at the indicated drug concentration for 14 days using the Click-IT EdU staining kit from life-technologies (Thermo-Fisher, Grand Island, NY); manufacturer's instructions were followed. Data was acquired on a 4-color Gallios flow cytometer (Beckman Coulter) and analyzed using Kaluza software.

*tPTEN<sup>-/-</sup> cell line KO99L:* *Pten*-deficient mice (*tPTEN<sup>-/-</sup>*) were obtained by crossing mice carrying two *Pten* floxed alleles with proximal *lck* promoter-cre transgenic mice and subsequently characterized via PCR as previously described (Hagenbeek et al., 2004). Mice and derived *tPTEN<sup>-/-</sup>* cell line KO99L was established as previously described (Rosilio et al., 2015). The murine KO99L cell line was grown in RPMI 1640 medium supplemented with 20% Fetal Calf-Serum and penicillin (50 units/mL), streptomycin (50 mg/mL) and sodium pyruvate (1.0 mM) Cell cultures were maintained at 37°C under 5% CO<sub>2</sub>.

*Measurement of KO99L cell metabolism (WST-1) and viability:* KO99L cells (40,000 cells per 100 µL) were incubated with compound **2** in a 96-well plate format for 48 h (37°C). Ten microliters of WST-1 reagent was added to each well and the absorbance of the formazan product was measured (490 nm). Each assay was performed in quadruplicate. Cells (5.0 x 10<sup>5</sup> cells per 2.0 mL) were incubated in a 6-well plate with indicated concentration of **2**, collected, washed twice with PBS and re-suspended with a staining solution containing DAPI (4',6'-diamidino-2-phenylindole) (0.5 µg/mL) and immediately analyzed by flow cytometry (MacsQuant Analyser, Miltenyi Biotech SA, Paris, France). Hence, cell viability was assessed using a WST-1 assay (evaluates mitochondrial dehydrogenase activity), whereas survival was quantified through DAPI incorporation.

### ***In vivo* PK and tissue distribution experiments**

*LC/MS-MS methods:* Liquid chromatography employed an Agilent Technologies, Zorbax extended-C18 50 x 4.6 mm, 5 micron column set at 40 °C with a flow-rate of 0.4 mL/min. The mobile phase consisted of A: 10 mM (NH<sub>4</sub>OAc), 0.1% formic acid in H<sub>2</sub>O, and B: 50:50 ACN:MeOH. The chromatography method used was 95% A for 0.5 min; ramped to 95% B at 7.0 min, held for 3.0 min, and then brought back to 95% A at 11.0 min and held for 1.5 min (12.5 min total run time). Compound (**2**) and deuterated GSK126-d7 used as an internal standard were observed via electro-spray ionization positive ion mode (ESI+) using the following conditions: i) an ion-spray voltage of 5500 V; ii) temperature, 450 °C; iii) curtain gas (CUR; set at 10) and Collisionally Activated Dissociation (CAD; set at 12) gas were nitrogen; iv) Ion Source gas one (GS1) and two (GS2) were set at 30; v) entrance potential was set at 10 V; vi) quadruple one (Q1) and (Q3) were set on Unit resolution; vii) dwell time was set at 200 msec; and viii) declustering potential (DP), collision energy (CE), and collision cell exit potential (CXP) are voltages (V). Samples (10 µL) were analyzed by LC/MS-MS: Compound (**2**) 563.5 → 255.3 m/z, DP (56), CE (61), CXP (16); GSK126-d7 IS 534.4 → 375.3 m/z, DP = (86), CE (35), CXP (10). The supplementary materials section also includes MS/MS and LC/MS-MS examples of **2** and internal standard.

*Sprague-Dawley Rat tissue distribution and Pharmacokinetic Studies:* The *in vivo* experiments were performed at East Tennessee State University – Quillen College of Medicine – in an AAALAC accredited facility. All procedures were reviewed and approved by the ETSU Committee on Animal Care; all research procedures adhered to the 'Principles of Laboratory Animal Care' (NIH publication #85-23, revised in 1985). Male Sprague-Dawley rats were purchased from Harlan World Headquarters (Indianapolis, Indiana,

USA), acclimated to the new surroundings (one week) and housed in groups of three at  $22 \pm 1$  °C and  $55 \pm 15\%$  humidity with 12 h dark light cycles. All animals had free access to water, but were fasted with access to water  $14 \pm 2$  h prior to dosing in cages with bedding. Animals were dosed in the morning, 2-3 h after the start of a light cycle. Fasted animals ( $284 \pm 21$  g) were dosed via ophthalmic venous plexus (orbital sinus) using a 1.0 mL disposable syringe with a 27G needle. Ophthalmic venous plexus doses were prepared immediately prior to dosing as aqueous solutions containing 10% DMSO; these rats were anaesthetized with isoflurane and subsequently infused (300  $\mu$ L over  $< 30$  s) with corresponding drug solution via the ophthalmic venous plexus (orbital sinus). Using tail-vein collection (the anterior portion was transected, 2-3 mm), blood samples (125  $\mu$ L) were collected using mini-capillary blood collection tubes containing EDTA dipotassium salt (SAFE-T-FILL®; RAM Scientific Inc., Yonkers, NY, USA). Animals administered via an orbital sinus dose had blood samples collected at time (OSD experiment one): 2, 5, 10, 15, 35, 48, 60 (1.0 h), 90, 120 (2.0 h), 180 (3.0 h), 210, and 240 min (4.0 h) post-dose; whereas, OSD experiment two: 5, 15, 30 min, and then at 1, 2, 4, 6, 8, 10, 12, 14, 24, 28 and 32 h post-dose. When the tissue distribution experiments were performed, animals were sacked (CO<sub>2</sub>) and blood, brains, kidneys, and livers were individually harvested and immediately frozen and stored ( $-80 \pm 10$  °C) until sample preparation and subsequent LC/MS-MS analysis. Control rat blood (K2 EDTA) and tissues (brains, kidneys and livers) were used to prepare standard curves from different biological matrices. Control and sample tissues were homogenized, for every 1.0 g tissue, 2.0 mL PBS (phosphate buffer saline; pH 7.4) was used. Standard curves (SC) were prepared by addition with thorough mixing of various aqueous drug solutions (50  $\mu$ L) into control blood or control homogenate (950  $\mu$ L); these were diluted serially to produce SC and QC

(quality control) samples. These samples were immediately frozen and stored ( $-80 \pm 10$  °C), undergoing one freeze thaw cycle as per the actual samples, until sample preparation and subsequent LC/MS-MS analysis. To analyze, blood samples (tissues samples) were removed in sets from the freezer and allowed to thaw on the benchtop (15 – 20 min) until signs of being thaw were obvious upon visual inspection, but were still cold. The blood samples were vortex mixed (5 sec), the caps opened and extraction solution (250  $\mu$ L) added, re-capped, vortex mixed (5 s), sonicated in water bath (5 min), vortex mixed (5 s) again, and then centrifuged (10,000 rpm; 10 min) using an Eppendorf mini-spin centrifuge (Hamburg, Germany). The extraction solution was prepared by mixing water (100 mL) with MeOH:acetonitrile (1:1; 300 mL) and spiking with stock internal standard DMSO solution. The supernatants were transferred into individual wells of a 96-well plate, placed into the LEAP auto-sampler cool-stack ( $8.0 \pm 0.1$  °C) and immediately analyzed via LC/MS-MS. In the case of the tissues, homogenates were prepared as per the standard curves, on a 1.0 g to every 2.0 mL PBS ratio; complete tissues were homogenized and samples were collected in triplicates and extracted in a 1:2 sample:extraction solution format as previously described. The individual standard curves (blood, brain, kidney and liver) were used to determine the apparent drug concentrations from the biological samples.

### *Software and statistics*

Pharmacokinetic (PK) data were computed using non-compartmental analysis model via linear trapezoidal rule via software program WinNonlin® (Phoenix Pharsight v6.3). Analyst 1.4.2 was used for LC/MS-MS data acquisition. Prism 4.02™ (GraphPad Software, Inc.; San Diego, CA) was used to graph and perform statistical analysis. Chemical structures were prepared using ChemBioDraw Ultra 12.0 (CambridgeSoft;

Cambridge, MA). The statistical differences in **Figures 3A, 3B, 3C, 4A and 4B** were compared using one-way analysis of variance followed by a Dunnett's multiple comparison test; ns =  $p > 0.5$ ; \* =  $p < 0.5$ ; \*\* =  $p < 0.01$ .

### ***Acknowledgments***

KA, KV, and MFW conducted chemical synthesis. JW, PJR and MFW designed and conducted *in vivo* experiments. We wish to thank Dr. Gregory A. Hanley at ETSU for his assistance to JW regarding *in vivo* orbital sinus dosing. The presented research utilized services of the Medicinal Chemistry Core Facility (MCCF) housed within the Department of Pharmaceutical Sciences (DOPS). Dr. K. Bernt commissioned the MCCF to prepare compound **2** and was supported by the Department of Pediatrics, University of Colorado Anschutz medical campus. Dr. Bernt's laboratory performed *in vitro* MLL-rearranged and non-MLL rearranged cell line experiments, but requested to merely be acknowledged in the current work. MN and JFP performed the experiments on KO99L cells and analyzed those data. MFW performed the Bioanalytical LC/MS-MS work. Lastly, the MCCF receives funding via CCTSI, an institute at the University of Colorado Denver supported in part by NIH/NCATS Colorado CTSI Grant Number UL1TR001082.

## References

- Anglin, J. L.; Deng, L.; Yao, Y.; Cai, G.; Liu, Z.; Jiang, H. 2012. Synthesis and structure-activity relationship investigation of adenosine-containing inhibitors of histone methyltransferase DOT1L. *J Med Chem.*, 55:8066-8074.
- Basavapathruni, A.; Olhava, E. J.; Daigle, S. R.; Therkelsen, C. A.; Jin, L.; Boriack-Sjodin, P. A. 2014. Nonclinical pharmacokinetics and metabolism of EPZ-5676, a novel DOT1L histone methyltransferase inhibitor. *Biopharm Drug Dispos.*, 35:237-252.
- Bernt, K. M.; Zhu, N.; Sinha, A. U.; Vempati, S.; Faber, J.; Krivtsov, A. V. 2011. MLL-rearranged leukemia is dependent on aberrant H3K79 methylation by DOT1L. *Cancer Cell.*, 20:66-78.
- Bitoun, E.; Oliver, P. L.; Davies, K. E. 2007. The mixed-lineage leukemia fusion partner AF4 stimulates RNA polymerase II transcriptional elongation and mediates coordinated chromatin remodeling. *Hum. Mol. Gen.*,16:92-106.
- Chang, M. J.; Wu, H.; Achille, N. J.; Reisenauer, M. R.; Chou, C. W.; Zeleznik-Le, N. J. 2010. Histone H3 lysine 79 methyltransferase Dot1 is required for immortalization by MLL oncogenes. *Cancer Res.*, 70:10234-10242.
- Chen, L.; Deshpande, A. J.; Banka, D.; Bernt, K. M.; Dias, S.; Buske, C. 2013. Abrogation of MLL-AF10 and CALM-AF10-mediated transformation through genetic inactivation or pharmacological inhibition of the H3K79 methyltransferase Dot1l. *Leukemia.*, 27:813-22.
- Chen, C-W.; Kocke, R.P.; Sinha, A.U.; Deshpande, A.J.; Zhu, N.; Eng, R.; Doench, J.G.; Xu, H.; Chu, S.H.; Qi, J.; Wang, X.; Delaney, C.; Bernt, K.M.; Root, D.E.; Hahn, W.C.; Bradner, J.E.; Armstrong, S.A. 2015. DOT1L inhibits SIRT1-mediated epigenetic silencing to maintain leukemic gene expression in MLL-rearranged leukemia. *Nature Medicine.*, 21: 335-343.
- Daigle, S. R.; Olhava, E. J.; Therkelsen, C. A.; Majer, C. R.; Sneeringer, C. J.; Song, J. 2011. Selective killing of mixed lineage leukemia cells by a potent small-molecule DOT1L inhibitor. *Cancer Cell.*, 20:53-65.
- Daigle, S. R.; Olhava, E. J.; Therkelsen, C. A.; Basavapathruni, A.; Jin, L.; Boriack-Sjodin, P. A. 2013. Potent inhibition of DOT1L as treatment of MLL-fusion leukemia. *Blood.*, 122:1017-1025.
- Deshpande, A. J.; Chen, L.; Fazio, M.; Sinha, A. U.; Bernt, K. M.; Banka, D. 2013. Leukemic transformation by the MLL-AF6 fusion oncogene requires the H3K79 methyltransferase Dot1l. *Blood.*, 121:2533-2541.
- Dlagic, M. 2001. Chromatin silencing protein and pachytene checkpoint regulator Dot1p has a methyltransferase fold. *Trends Biochem Sci.*,26:405-407.
- Ho, L. L.; Sinha, A.; Verzi, M.; Bernt, K. M.; Armstrong, S. A.; Shivdasani, R. A. 2013. DOT1L-mediated H3K79 methylation in chromatin is dispensable for Wnt pathway-specific and other intestinal epithelial functions. *Mol Cell Biol.*, 33:1735-1745.
- Jo, S. Y.; Granowicz, E. M.; Maillard, I.; Thomas, D.; Hess, J. L. 2011. Requirement for Dot1l in murine postnatal hematopoiesis and leukemogenesis by MLL translocation. *Blood.*, 117:4759-4768.
- Jones, B.; Su, H.; Bhat, A.; Lei, H.; Bajko, J.; Hevi, S. 2008. The histone H3K79 methyltransferase Dot1L is essential for mammalian development and heterochromatin structure. *PLoS Genet.*, 4:e1000190.
- Klaus, C.R.; Iwanowicz, D.; Johnston, D.; Campbell, C.A.; Smith, J.J.; Moyer, M.P.; Copeland, R.A.; Olhava, E.J.; Scott, M.P.;

- Pollock, R.M.; Daigle, S.R.; Raimondi, A. 2014. DOT1L Inhibitor EPZ-5676 Displays Synergistic Antiproliferative Activity in Combination with Standard of Care Drugs and Hypomethylating Agents in MLL-Rearranged Leukemia Cells. *JPET.*, 350: 646-656.
- Mahmoudi, T.; Boj, S. F.; Hatzis, P.; Li, V. S.; Taouatas, N.; Vries, R. G. 2010. The leukemia-associated Mllt10/Af10-Dot1l are Tcf4/beta-catenin coactivators essential for intestinal homeostasis. *PLoS Biol.*, 8:e1000539.
- Min, J.; Feng, Q.; Li, Z.; Zhang, Y.; Xu, R. M. 2003. Structure of the catalytic domain of human DOT1L, a non-SET domain nucleosomal histone methyltransferase. *Cell.*, 112:711-723.
- Mueller, D.; Bach, C.; Zeisig, D.; Garcia-Cuellar, M. P.; Monroe, S.; Sreekumar, A. 2007. A role for the MLL fusion partner ENL in transcriptional elongation and chromatin modification. *Blood.*, 110:4445-4454.
- Mueller, D.; Garcia-Cuellar, M. P.; Bach, C.; Buhl, S.; Maethner, E.; Slany, R. K. 2009. Misguided transcriptional elongation causes mixed lineage leukemia. *PLoS Biol.* 7:e1000249.
- Ng, H. H.; Feng, Q.; Wang, H.; Erdjument-Bromage, H.; Tempst, P.; Zhang, Y. 2002. Lysine methylation within the globular domain of histone H3 by Dot1 is important for telomeric silencing and Sir protein association. *Genes Dev.*, 16:1518–1527.
- Nguyen, A. T.; He, J.; Taranova, O.; Zhang, Y. 2011(a). Essential role of DOT1L in maintaining normal adult hematopoiesis. *Cell Res.*,21:1370-1373.
- Nguyen, A. T.; Taranova, O.; He, J.; Zhang, Y. 2011(b). DOT1L, the H3K79 methyltransferase, is required for MLL-AF9-mediated leukemogenesis. *Blood.*, 117:6912-6922.
- Nguyen, A. T.; Xiao, B.; Neppl, R. L.; Kallin, E. M.; Li, J.; Chen, T. 2011(c). DOT1L regulates dystrophin expression and is critical for cardiac function. *Genes Dev.*, 25:263-274.
- Nguyen, A. T.; Zhang, Y. 2011(d). The diverse functions of Dot1 and H3K79 methylation. *Genes Dev.*, 25:1345-58. doi: 10.1101/gad.2057811
- Okada, Y.; Feng, Q.; Lin, Y.; Jiang, Q.; Li, Y.; Coffield, V. M. 2005. hDOT1L links histone methylation to leukemogenesis. *Cell.*, 121:167-78.
- Olhava, J.E.; Chesworth, R.; Kuntz, W.K.; Richon, M.V.; Pollock, M.R. 2012. International Application Published Under The Patent Cooperation Treaty (PCT). WO 2012/075381 A1.
- Olhava, J.E.; Chesworth, R.; Kuntz, W.K.; Richon, M.V.; Pollock, M.R.; Daigle, R.S. 2014(a). International Application Published Under The Patent Cooperation Treaty (PCT). WO 2014/039839 A1.
- Onder, T. T.; Kara, N.; Cherry, A.; Sinha, A. U.; Zhu, N.; Bernt, K. M. 2012. Chromatin-modifying enzymes as modulators of reprogramming. *Nature.*, 483:598-602.
- Park, J. H.; Cosgrove, M. S.; Youngman, E.; Wolberger, C.; Boeke, J. D. 2002. A core nucleosome surface crucial for transcriptional silencing. *Nat Genet.*,32:273-279.
- Rosilio, C.; Nebout, M.; Imbert, V.; Griessinger, E.; Neffati, Z.; Benadiba, J.; Hagenbeek, T.; Spits, H.; Reverso, J.; Ambrosetti, D.; Michiels, J. F.; Bailly-Maitre, B.; Endou, H.; Wempe, M. F.; Peyron, J. F. 2015. Leukemia., in press. Dec 8. doi: 10.1038/leu.2014.338. [Epub ahead of print] PMID: 25482130.
- Sawada, K.; Yang, Z.; Horton, J. R.; Collins, R. E.; Zhang, X.; Cheng, X. 2004. Structure of the conserved core of the yeast Dot1p, a nucleosomal histone H3 lysine 79 methyltransferase. *J Biol Chem.*, 279:43296-43306.
- Segawa, H.; Fukasawa, Y.; Miyamoto, K.;

Takeda, E.; Endou, H.; Kanai, Y. 1999. Identification and functional characterization of a Na<sup>+</sup>-independent neutral amino acid transporter with broad substrate selectivity. *J Biol Chem.*, 274:19745-19751.

Steger, D. J.; Lefterova, M. I.; Ying, L.; Stonestrom, A. J.; Schupp, M.; Zhuo, D. 2008. DOT1L/KMT4 recruitment and H3K79 methylation are ubiquitously coupled with gene transcription in mammalian cells. *Mol Cell Biol.*, 28:2825-2839.

van Leeuwen, F.; Gafken, P. R.; Gottschling, D. E. 2002. Dot1p modulates silencing in yeast by methylation of the nucleosome core. *Cell.*, 109:745-56.

Wempe, M. F.; Lightner, J. W.; Miller, B.; Iwen, T. J.; Rice, P. J.; Wakui, A.; Anzai, N.; Jutabha, P.; Endou, H. 2012. Potent human uric acid transporter 1 inhibitors: in vitro and in vivo metabolism and pharmacokinetic studies. *Drug Design, Development and Therapy*, 6:323-339.

Yanagida, O.; Kanai, Y.; Chairoungdua, A.; Kim, D. K.; Segawa, H.; Nii, T.; Cha, S. H.; Matsuo, H.; Fukushima, J.; Fukasawa, Y.; Tani, Y.; Taketani, Y.; Uchino, H.; Kim, J. Y.; Inatomi, J.; Okayasu, I.; Miyamoto, K.; Takeda, E.; Goya, T.; Endou, H. 2001. Human L-type amino acid transporter 1 (LAT1): characterization of function and expression in tumor cell lines. *Biochim Biophys Acta.*, 1514:291-302.

Yang, L.; Lin, C.; Jin, C.; Yang, J. C.; Tanasa, B.; Li, W. 2013. lncRNA-dependent mechanisms of androgen-receptor-regulated gene activation programs. *Nature.*, 500:598-602.

Yu, W.; Chory, E. J.; Wernimont, A. K.; Tempel, W.; Scopton, A.; Federation, A. 2012. Catalytic site remodelling of the DOT1L methyltransferase by selective inhibitors. *Nat Commun.*, 3:1288.

Yu, W.; Smil, D.; Li, F.; Tempel, W.; Fedorov, O.; Nguyen, K. T. 2013. Bromo-

deaza-SAH: a potent and selective DOT1L inhibitor. *Bioorg Med Chem.*, 21:1787-1794.

## Supplementary Material Section

# DOT1L INHIBITOR EPZ-5676: SYNTHESIS, PHARMACOKINETIC AND TISSUE DISTRIBUTION STUDIES IN SPRAGUE-DAWLEY RATS

*Vijay Kumar<sup>a</sup>; Amit Kumar<sup>a</sup>; Janet W. Lightner<sup>b</sup>; Peter J. Rice<sup>a,b</sup>; Marielle Nebout<sup>c</sup>; Jean-Francois Peyron<sup>c</sup>; Michael F. Wempe<sup>a,d,\*</sup>*

\* Corresponding Author: Michael F. Wempe  
Michael F. Wempe, PhD  
michael.wempe@ucdenver.edu  
(T) 303-724-8982  
(F) 303-724-6148

<sup>a</sup>Department of Pharmaceutical Sciences, School of Pharmacy, University of Colorado Denver Anschutz Medical Campus, Aurora, CO 80045, USA

<sup>b</sup>Department of Pharmacology, East Tennessee State University Johnson City, TN 37614, USA

<sup>c</sup>INSERM, U1065, Centre Méditerranéen de Médecine Moléculaire (C3M), Equipe Inflammation, Cancer, Cellules Souches Cancéreuses, Nice, France.

<sup>d</sup>University of Colorado Cancer Center, University of Colorado Denver, Aurora, Colorado 80045, USA

Email addresses, co-authors: Vijay Kumar – vijay.kumar@ucdenver.edu; Amit Kumar – amit.2.kumar@ucdenver.edu; Janet W. Lightner – lightner@mail.etsu.edu; Peter J. Rice – peter.rice@ucdenver.edu; Marielle Nebout – marielle.nebout@unice.fr; Jean-Francois Peyron – jean-francois.peyron@unice.fr.

*Keywords—Dot1L Inhibitor; EPZ-5676; Rat Pharmacokinetic Study*

---

\* Corresponding author. Tel.: 303-724-8982; fax: 303-724-6148; e-mail: michael.wempe@ucdenver.edu

**S-Figure 1** LC/MS-MS of Dot1L inhibitor compound 2 and internal standard, GSK126-d7

